Physics of the Earth and Planetary Interiors 356 (2024) 107268

Contents lists available at ScienceDirect

Physics of the Earth and Planetary Interiors

journal homepage: www.elsevier.com/locate/pepi

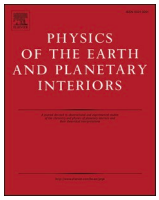

Reinvestigating the Dufek Intrusion, through joint gravity and magnetic models

Tom A. Jordan *, Teal R. Riley

British Antarctic Survey, High Cross, Madingley Road, Cambridge CB3 0ET, UK

ARTICLE INFO

Keywords:
Layered intrusion
Antarctica
Jurassic
Ferrar Large Igneous Province
Magma emplacement

ABSTRACT

The Dufek layered mafic intrusion represents the only exposed, deep-seated, part of the Ferrar Large Igneous Province, which extends >3500 km across Antarctica and into parts of Tasmania and New Zealand. The Dufek Intrusion is in a key position at the boundary between the Jurassic Weddell Sea Rift System and the East Antarctic Craton. It may have been a conduit for some of the Ferrar magmas, or a deep-seated equivalent to the shallower sills seen in other sectors of Antarctica. Although a significant intrusion, equivalent at least to the Stillwater complex in the USA, its true scale and geometry, along with the relative timing of emplacement is disputed. We present new 3D models of gravity and magnetic data which constrain the geometry of the intrusion, show how separate lobes of the intrusion are linked and identify a possible extension of the intrusion to the east. We also discuss the implications for how the intrusion may have been emplaced.

1. Introduction

1.1. Layered intrusions and large igneous provinces

Layered mafic intrusions are large magmatic bodies where flow within the magma chamber, coupled with on-going crystallisation, crystal settling and other magmatic processes, leads to development of crystal fabrics visually like those in sedimentary rocks. The origins of layering are complex but can be broadly divided into two types: i) dynamic processes, such as magmatic flow, and ii) non-dynamic processes, including differing rates of crystal nucleation and growth developing in non-flow conditions. Overlap between these two types can develop in an intrusive body over time. Layered intrusions reveal how mafic magmatic systems evolve with time and are of interest globally as a source of platinum group elements. The largest known layered intrusion is the ~300 × 400 km Archean Bushveld complex of South Africa which has a thickness of ~9 km (Cole et al., 2021). Other well-known but smaller layered intrusions include the Neoarchean Stillwater complex of the USA, which geophysical data indicate extends over an area of 64 × 32 km, with a thickness of ~9 km (Finn et al., 2020), and the ~55 Ma Skaergaard intrusion (Greenland) which is ~11 × 8 km across and ~4 km thick (Nielsen, 2004). The large volume of magma required to facilitate development of the layered structures is consistent with the observation that many layered intrusions, such as Skaergaard, are part of wider large igneous provinces (LIPs).

1.2. Geological setting and age of the Dufek intrusion

The Dufek layered Intrusion was emplaced into folded Cambrian to Devonian sediments in the northern part of the Pensacola Mountain Range (Fig. 1a). This location is close to the tectonic boundary between East and West Antarctica, which is proposed to follow the Pagano Shear Zone (Jordan et al., 2013). The oldest sedimentary sequences show more intense folding developed during the ~500 Ma Ross Orogeny (Cawood, 2005). Younger (Devonian to Permian) sequences, including the widespread Dover Sandstone are separated from the older sequences by angular unconformities and show more limited deformation into generally broad low-angle folds (Curtis et al., 2004).

The Dufek Intrusion is exposed in two adjacent mountain ranges, the smaller western Dufek Massif (55 × 10 km) and the larger eastern Forrestal Range (110 × 26 km) (Fig. 1). These mountain ranges have peaks over 1700 m high, run broadly N/S and are separated by the ~45 km wide Sallee Snow Field, an icy plateau 1–1.3 km thick with a surface altitude of ~1100 m. The contact between the Intrusion and the surrounding country rock is largely ice covered. However, a high angle intrusive contact with the Dover Sandstone outcrops at Mount Lechner in the Forrestal Range (Ford, 1976), with a dip of 45° to the southeast (Semenov et al., 2014). Other outcropping sediments in this area lie in

* Corresponding author.
E-mail address: tomj@bas.ac.uk (T.A. Jordan).

https://doi.org/10.1016/j.pepi.2024.107268
Received 1 July 2024; Received in revised form 27 September 2024; Accepted 1 October 2024
Available online 2 October 2024

the thermal aureole (Ford, 1976). The layering within the intrusion generally shows a 5–10 degree south-eastward dip, implying the Aughenbaugh Gabbro exposed in the Dufek Massif forms the basal part of the intrusion, while the Saratoga Gabbro and overlying Lexington Granophyre in the Forrestal Range from the stratigraphically shallower part (Ford, 1976) (Fig. 2c).

Geochemically the Dufek Massif and Forrestal Range parts of the intrusion show distinct but overlapping patterns. The whole rock Fe/Mg ratios increase towards the presumed upper part of the intrusion, reflecting progressive Fe enrichment, with the Forrestal Range showing the highest values (Ford, 1976). Petrological observations show that oxide minerals, such as magnetite, only become an abundant phase towards the upper levels of the Dufek Massif, but are found throughout the Forrestal Range (Himmelberg and Ford, 1977). Such progressive change in geochemistry has been attributed to fractional crystallisation of a single large magmatic body (Semenov et al., 2014). $^{87}Sr/^{86}Sr$ and $\delta^{18}O$ isotopic values across the two exposed parts of the intrusion also show distinct but overlapping patterns, however, these are attributed to variable amounts of crustal contamination and pulses of new magma, suggesting a more complex emplacement mechanism in a dynamic setting (Kistler et al., 2000). A more complex growth pattern driven by multiple injections of magma is also suggested by other petrological (Carnes et al., 2011) and isotopic studies (Dunlop et al., 2016). A complex emplacement history with the rocks of the Dufek Massif emplaced at shallow depth and representing a separate intrusion from the Forrestal Range are also suggested by some paleomagnetic studies (Gee et al., 2009).

Geochemical and mineralogical characteristics influence the bulk rock properties of density and susceptibility which are important for understanding and interpreting the geophysical properties of the intrusion. As magnetite is known to be a key contributor to magnetic susceptibility it is unsurprising that the rocks of the Forrestal Range, where magnetite is abundant, consistently show higher susceptibility values than those of the Dufek Massif (Beck, 1972). This is confirmed by data from the Byrd Polar Rock repository (Fig. 2a and Table 1) which shows the Aughenbaugh Gabbro of the Dufek Massif has an average susceptibility of 237×10^{-5} SI ($n = 605$) while the Saratoga Gabbro forming the bulk of the Forrestal Range shows a mean susceptibility of 6692×10^{-5} SI ($n = 995$) (Fig. 2c). Within the Forrestal Range the most extreme susceptibility values (>20,000 $\times$ 10^{-5} SI) are found at altitudes of >1300 m and may reflect sampling of distinct magnetite rich layers. Rock density is also a function of geochemical composition and has been shown to vary in direct proportion to the volume percentage of pyroxene (Ford and Nelson, 1972). The average measured density of the Dufek Massif, weighted for the relative abundance of the different rock types, is ~2.95 g/cc while the Forrestal Range has a slightly higher average density of 3.03 g/cc (Ford and Nelson, 1972) (Fig. 2c).

Several studies have investigated the age of the Dufek Intrusion. A U—Pb age of 183.9 ± 0.3 Ma has been reported for the capping Lexington Granophyre of the Forrestal Range and a 182.7 ± 0.4 Ma age for a late stage felsic dyke (Minor and Mukasa, 1997). Higher precision ages of magmatism from across the entire Ferrar LIP have also been determined, with weighted mean ages of 182.700 ± 0.045 Ma and 182.629 ± 0.029 Ma for capping granophyres from the Forrestal Range at Mount Zirzow and Mount Lechner respectively (Burgess et al., 2015). The emplacement of the Dufek Intrusion was therefore synchronous with the

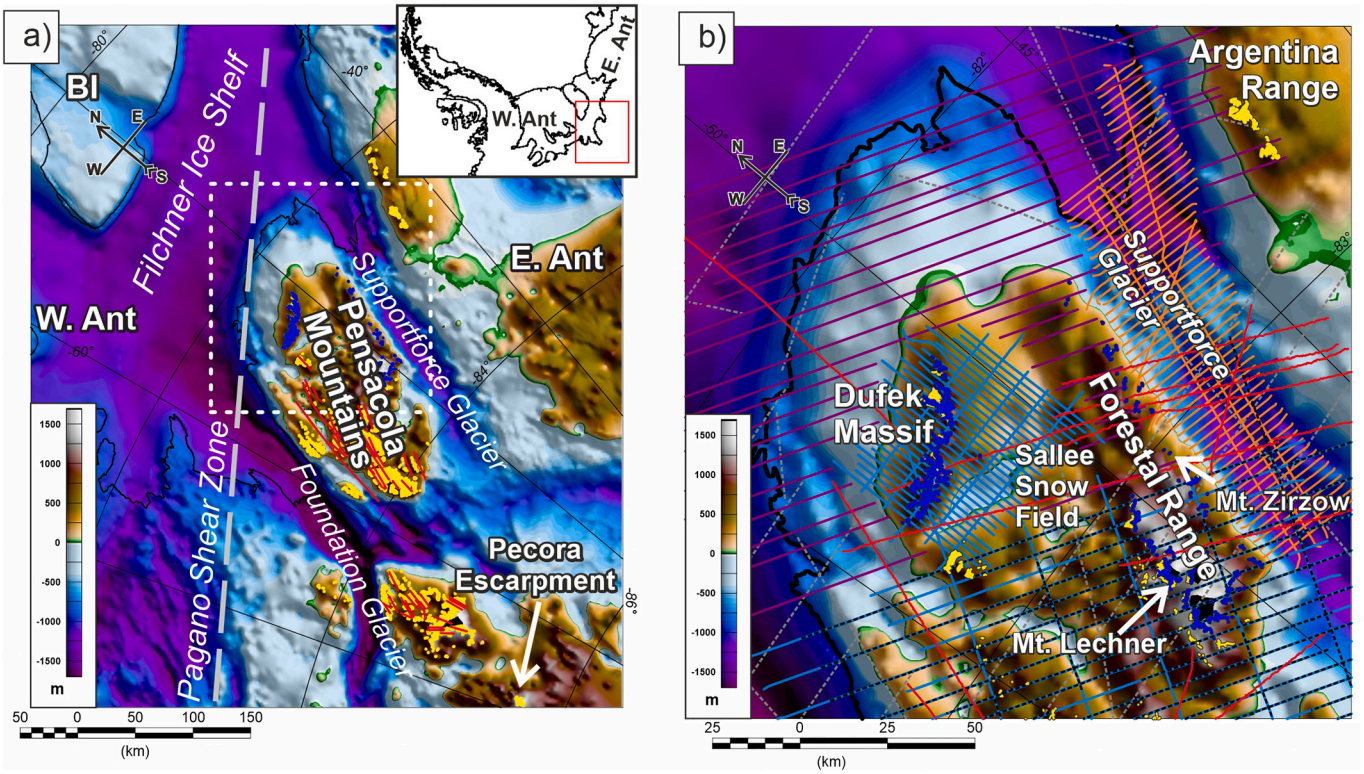

Fig. 1. Location map. a) Subglacial topography of the Pensacola Mountains and surrounding glaciers from Bedmachine Antarctica (Morlighem et al., 2020). Blue lines show outcropping Dufek Intrusion while yellow lines mark other rock outcrops from the SCAR Geomap (Cox et al., 2023). Red lines indicate faults/lineations (Curtis, 2002; Storey et al., 1996). Black lines mark coast/grounding line at edge of ice shelf. Dashed box locates (b). Inset shows study area in Antarctic context. BI is Berkner Island, E. Ant and W. Ant are East and West Antarctica respectively. b) Survey lines and bed topography of study area. Magnetic data from ADMAP2 (Golynsky et al., 2018) and the 2016 Foundation Ice Shelf Survey (FISS) (Jordan et al., 2021) as solid lines. Red = SPRI 1978, Purple = USSR 1978, Blue = BAS Dufek 1999, Orange = BAS FISS 2016. Note gaps in older magnetic line data where more modern surveys provide data with higher navigational accuracy. Gravity data as dashed lines. Black = BAS gravity 1999 (Jones, 2020), Grey = OIB gravity (Tinto et al., 2010, updated 2019). (For interpretation of the references to colour in this figure legend, the reader is referred to the web version of this article.)

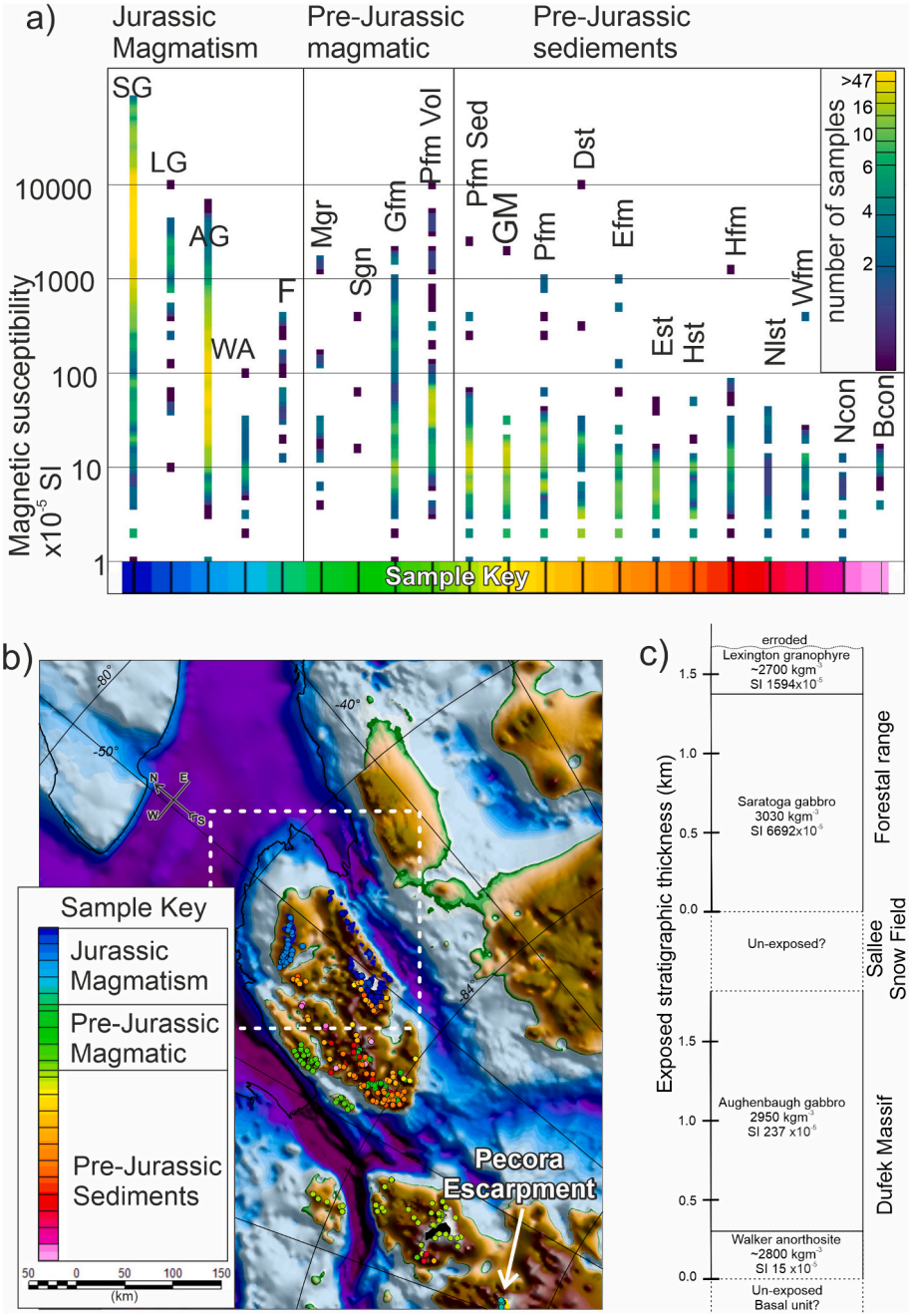

Fig. 2. Measured magnetic susceptibility values (The Polar Rock Repository (PRR), 2021). a) Visualization of susceptibility distribution for each geological formation in the study area. Full formation name and abbreviation given in Table 1. Jurassic magmatism includes Dufek Intrusion and samples of the Ferrar Dolerite at Pecora Escarpment. Sample Key indicates symbol colour on map in panel (b). Note log10 vertical scale used to show all samples. b) Spatial distribution of samples. Dashed white box locates Fig. 3. c) Presumed stratigraphic order and thickness, together with mean susceptibility and density for the Dufek Intrusion (Ford and Nelson, 1972; Semenov et al., 2014).

intrusion of mafic sills from the central Transantarctic Mountains (weighted mean age of 182.63 ± 0.30 Ma) and southern Victoria Land (weighted mean 182.636 ± 0.044 Ma). A more recent investigation using chemical abrasion ID-TIMS (VanTongeren et al., 2020) yielded weighted mean ages of 182.464 ± 0.030 Ma for the Dufek Massif and a marginally older weighted mean age of 182.646 ± 0.031 Ma for the presumed stratigraphically shallower Forrestal Range. The close but distinct ages for these samples could reflect differences in the time for different depths of the intrusion to cool to the zircon saturation temperature. Alternatively, similar out of sequence ages, i.e. where younger rocks are found in a stratigraphically lower position, have been observed in the Bushveld intrusion (Mungall et al., 2016; Scoates et al., 2021), where the dating has led to the suggestion that layered intrusions were not large magma chambers, but rather the product of repeated intrusions of sill like bodies, which may actually show progressive younging downwards. Elsewhere in the Ferrar LIP, the layered felsic-intermediate intrusion at Butcher Ridge of the central Transantarctic Mountains has an age of c. 182.4 Ma, akin to the Ferrar Province sills and Dufek Intrusion (Nelson et al., 2019).

1.3. *Previous geophysical interpretation of the Dufek Intrusion*

Both the areal extent and the detailed geometry of the Dufek Intrusion are uncertain due to the sparse, or absent outcrop around and

Table 1
Summary of measured susceptibility values (The Polar Rock Repository (PRR), 2021). Abbreviated names (Abrv.) match abbreviations in Fig. 2a. Number of samples (*n*) from a total of 2987 samples.

			Susceptibility x10^{-5} (SI)			
Formation name	Abrv.	*n*	min	max	mean	Stdev
Saratoga Gabbro	SG	995	1	80,285	6692	10,528
Lexington Granophyre	LG	49	11	9699	1594	1559
Aughenbaugh Gabbro	AG	606	0	7075	237	595
Walker Anorthosite	WA	32	2	100	15	18
Ferrar Dolerite	F	22	13	438	135	141
Median Granite	Mgr	21	4	1760	244	528
Serpan Gneiss	Sgn	3	15	414	162	219
Gambacorta Formation	Gfm	133	1	1798	181	357
Patuxent Formation (volcanic)	Pfm Vol	141	3	9890	294	1100
Patuxent Formation (sediments)	Pfm Sed	173	0	2400	35	189
Gale Mudstone	GM	140	0	2200	26	185
Pecora Formation	Pfm	139	0	1000	42	150
Dover Sandstone	Dst	138	0	9370	75	798
Elbow Formation	Efm	92	1	992	47	166
Elliott Sandstone	Est	74	0	47	8	7
Heiser Sandstone	Hst	65	0	50	7	10
Hannah Ridge Formation	Hfm	54	0	1200	38	162
Nelson Limestone	Nlst	45	0	42	9	13
Wiens Formation	Wfm	34	0	364	30	85
Neith Conglomerate	Ncon	16	1	12	5	4
Brown Ridge Conglomerate	Bcon	15	4	17	9	4

between the Dufek Massif and Forrestal Range and to the north (Fig. 1b). The rock outcrop has an area of ~107 km^2 of Jurassic igneous rocks (Cox et al., 2023), which at a minimum gives a buried area of 2202 km^2 enclosed by the known exposures. The Dufek Intrusion has been linked to magnetic anomalies ~200 km north on Berkner Island, based on reconnaissance aeromagnetic data (Behrendt et al., 1980) indicating a much larger areal extent of ~50,000 km^2. The Berkner Island anomalies were subsequently re-interpreted as a distinct basement block, separated along a dextral fault away from previously coincident basement interpreted beneath the Support Force Ice Stream (Ferris et al., 1998). Other long wavelength anomalies in the region with lower amplitudes are interpreted to be basement, or potentially, offshore to the west, other unrelated intrusions (Ferris et al., 1998), while high frequency features were interpreted as a suite of Jurassic or Cambrian dykes (Ferris et al., 2003). Such re-interpretation of the main anomalies gave a smaller area for the combined Dufek and Forrestal intrusion of 6600 km^2. In addition to arguing for a smaller size, it was argued that the Dufek and Forrestal bodies were distinct based on the differing magnetic trends and modelled susceptibilities seen in the two areas (Ferris et al., 1998). The Dufek Intrusion was interpreted to be older and less extensive, while the younger Forrestal body was split into distinct eastern and western bodies by subsequent faulting.

2. Methods for re-analysis

2.1. Input geophysical data

Our study of the Dufek Intrusion is based on analysis and interpretation of associated airborne magnetic and gravity data. No consistent aerogeophysical survey covers the entire intrusion, so we have produced data compilations based on existing published datasets.

The aeromagnetic compilation is primarily based on data available through the ADMAP compilation (Golynsky et al., 2018). Additional aeromagnetic data, collected opportunistically during an aerogeophysical survey of the Filchner Ice Shelf region (FISS), was also included, giving enhanced resolution over the adjacent Support Force Glacier (Jordan et al., 2021). All the available line magnetic data were combined into a single database and an initial assessment made of the data quality. In some areas, where older surveys conducted prior to the advent of GPS navigation overlapped more modern surveys, identifiable magnetic anomalies appeared to be latterly offset by up to 5 km. We therefore only included the older datasets in the final gridded magnetic data product where there was no more recent data, or where levelling could provide an acceptable match. After data selection we carried out statistical levelling to produce a consistent aeromagnetic data set (Fig. 3a).

The airborne gravity data comes primarily from a survey flown in 1998/99 by the British Antarctic Survey, collecting magnetic, gravity and radar data. The gravity data was collected using a LaCoste and Romberg air-sea gravity system in a ZLS stabilised platform (Jones, 2020). The gravity dataset is restricted to the southern Forrestal Range (Fig. 1b). The LaCoste and Romberg data were corrected to free air anomalies using standard processing steps (Jones and Johnson, 1995), including application of a 9 km low pass filter. The free air gravity dataset shows a relatively large crossover error of 9.1 mGal, likely reflecting the quality of the available GPS processing, coupled with non-ideal flying conditions. Three additional gravity profiles across the Forrestal Range were collected by Operation Ice Bridge, in 2012. This more recent gravity dataset has an estimated error of ~1 mGal, based on internal crossover analysis in other areas (Tinto et al., 2010, updated 2019). These two datasets were continued to a common altitude of 2500 m, and statistically levelled, giving a relatively smooth gravity anomaly field, and a residual standard deviation at the crossover points of 5.91 mGal (Fig. 5a).

2.2. Digital enhancement

To assess the areal extent of the Dufek intrusion we applied the horizontal tilt angle (TDX) digital enhancement using the gradients calculated from our magnetic compilation (Cooper and Cowan, 2006). This enhancement is calculated as the inverse tangent of the total horizontal gradient of the magnetic field, normalised by the vertical gradient of the field. The resulting enhancement shows peaks over anomaly edges, assuming vertical contacts between magnetic sources. An advantage of this method is that it identifies source edges irrespective of anomaly amplitude which varies significantly across the study area. The depth of the sources for the Dufek Intrusion was evaluated using the tilt depth method. This uses the tilt angle calculated from the inverse tangent of the vertical gradient of the magnetic field normalised by the total horizontal gradient of the field. The zero value for the tilt angle corresponds to the source edge, and the distance to pairs of positive and negative tilt angle contours is proportional to the source depth (Salem et al., 2007). We compared depths based on the distance from the zero contour to the adjacent +/− 30° contours, discarding depths where the estimates were inconsistent, or where the directions to the adjacent contours were not approximately anti-parallel to isolate the most robust depth estimates (Jordan and Becker, 2018).

Free air gravity anomalies are dominated by the signature of the terrain, rather than the underlying geology, due to the large density contrast at the rock/ice or rock/air boundary. The Bouguer correction is a gravitational model for the impact of the topography and ice calculated using standard reference densities of 915 kgm^{-3}, 1028 kgm^{-3} and 2670 kgm^{-3} for ice, water and rock respectively. The correction was calculated in 3D using a prism based approach (von Frese et al., 1981), at a uniform observation altitude of 2500 m. Subtraction of this correction from the free air data, also continued to 2500 m altitude, strips out the impact of topography and ice filled valleys from the observed gravity signal, revealing density variations in the rocks beneath. Where the reference density used is incorrect, e.g. a mountain of dominantly gabbroic composition may have a real density > 2670 kgm^{-3}, the residual anomaly after the Bouguer correction will contain a gravity anomaly proportional to the error in density. This anomaly is then factored into subsequent models and analysis. Although short wavelength gravity features associated with topography are largely

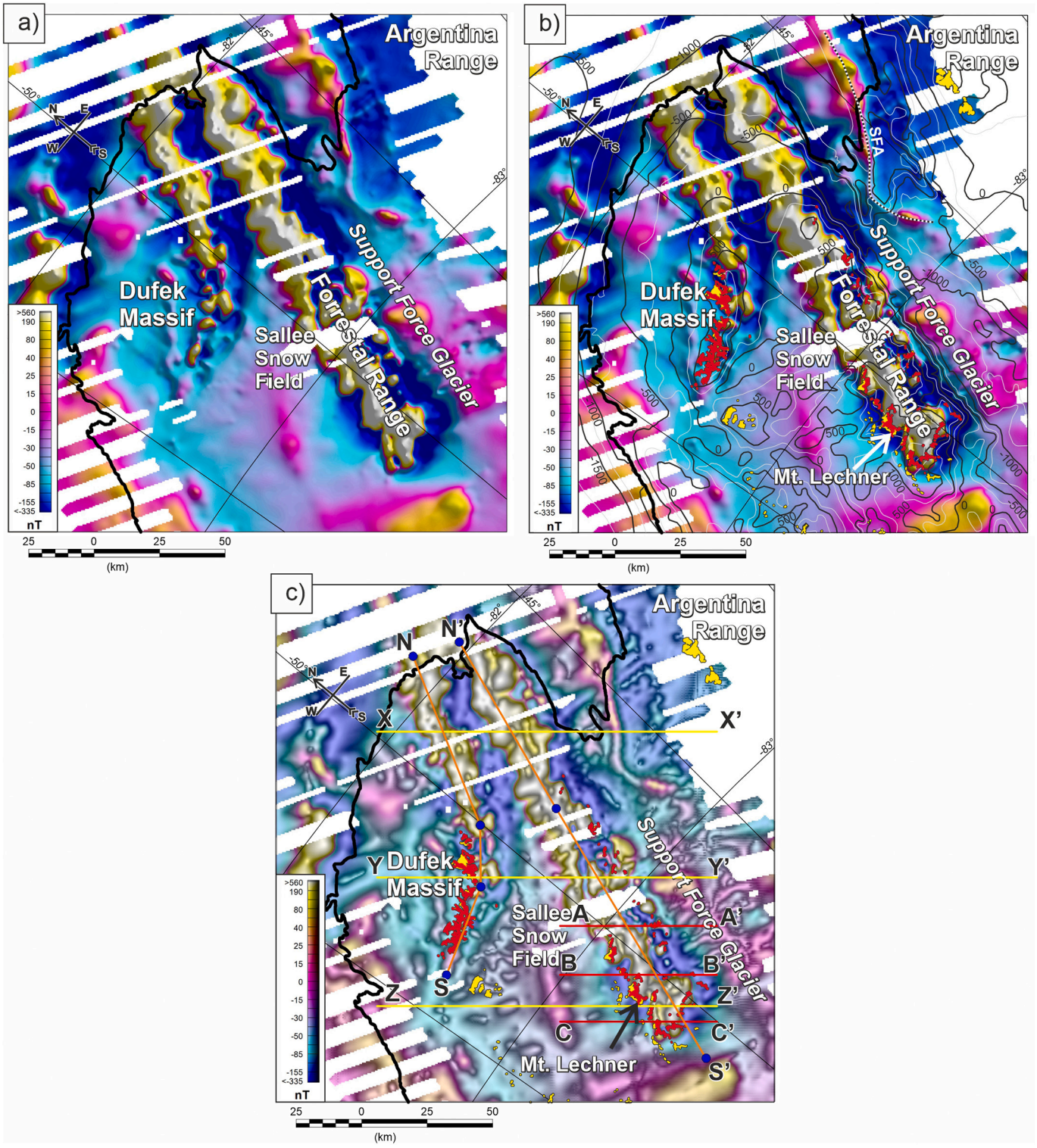

Fig. 3. Aeromagnetic anomaly map over Dufek Intrusion. a) Reduced to the Pole aeromagnetic anomaly. b) Annotated magnetic anomaly map. Red and yellow areas locate Jurassic intrusive and other rock outcrops respectively. Contours (black and grey) show bedrock elevation from Bedmachine2. Dotted black and white line marks Support force Anomaly (SFA). c) Aeromagnetic anomaly from (a) with TDX enhancement of theoretical source edges. Grey/black shading indicates high TDX values locating source boundaries. Red and yellow lines show example profiles from joint local gravity/magnetic model (Fig. 7) and regional magnetic only model (Fig. 9) respectively. Orange lines show additional longitudinal sections of model shown in Fig. 10. Blue dots mark profile inflection points. Note linear banding apparent beneath the southern part of the Support Force Glacier is an artifact of incomplete levelling of the magnetic line data, due to a lack of tie lines in the underlying opportunistic magnetic dataset. (For interpretation of the references to colour in this figure legend, the reader is referred to the web version of this article.)

removed by the Bouguer correction, long wavelength gravity signatures due to variations in crustal thickness, for example due to isostatic compensation of surface topography and ice loads, are still present in the Bouguer gravity field. The gravity effect of a crustal model assuming Airy Isostatic compensation of the surface topography was therefore calculated assuming reference crust with a Moho at 31 km depth and an observation altitude of 2500 m. The resulting calculated gravity field was subtracted from the Bouguer anomaly, leaving the Airy isostatic residual. This residual anomaly is theoretically dominated by density variations in the upper crust, although deviations from the assumed method of isostatic compensation may be revealed as longer wavelength residual gravity anomalies.

Additional land gravity data collected in the 1960s (Behrendt et al., 1974) provide observations away from the main airborne surveys (Fig. 5d). The land free air gravity anomalies were corrected using the same Bouguer and Airy isostatic corrections as the airborne data. This is an approximation, as the airborne Bouguer correction is calculated at a fixed altitude. Continuation of the point free air data to the same altitude is not practical as full wavelengths of the gravity field are not captured in the original land surveys. However, we include the corrected land gravity data in our regional gravity compilation as it gives the most complete view of the regional gravity field.

2.3. Modelling

To assess the sub-surface structure and extent of the intrusive bodies we constructed 3D forward models, constrained by observed magnetic and, where available, gravity data. The software we used was "Interactive Gravity and Magnetic Application System" IGMAS+ software (v1.4.8707) (Goetze and Lahmeyer, 1988; Götze and Schmidt, 2010), currently maintained by GFZ Potsdam (Anikiev et al., 2020). During forward modelling the software calculates the 3D gravity and magnetic anomalies resulting from irregular shaped 3D polyhedra. The polyhedra are created using a series of 2D profiles intersecting known or expected interfaces/bodies. Nodes on the individual 2D profiles are linked between lines by a triangulation algorithm, creating the modelled 3D polyhedra. Additional bodies on two or more profiles can be added and their gravity and magnetic effects calculated. A visually optimal model is then constructed by moving nodes on the individual 2D sections and recalculating the 3D geometry and associated magnetic and gravity fields. As the model is a visual fit, the residual errors are relatively large. A better fitting model is possible, but would require additional complexity which is not justified given the uncertainties in the input data.

Two 3D models were constructed. The first joint model focused on the area where both gravity and magnetic data are available over the Forrestal Range. The input data for the modelling was the Airy isostatic gravity anomaly and levelled magnetic anomaly data, both continued to a constant altitude of 2500 m. The second model included the Dufek and Forrestal outcrops and the area enclosed by peaks in the TDX enhancement interpreted to mark the approximate edge of the intrusion. This wider model only considered magnetic data and aimed to constrain the regional form of the intrusion. The observation altitude for this model was extracted from the flight elevations reported for the magnetic dataset. To enable efficient calculation of both models the constraining data had a 2 km point spacing, sampled onto a regular mesh, based on the gridded data products (Fig. 3a and 4c). The 3D calculations were constrained by 2D model sections separated by 6 km. The base of the modelled bodies was initially assumed to be flat. Potential field data does not resolve the base of bodies well, so this simplified structure is assumed. Where the model required the bodies to be thicker, we aimed to maintain a simple basal geometry by minimising the number of additional basal nodes, but acknowledge that a more complex base may be present in reality. The magnetic model assumed an inclination of −68° and a declination of 19° corresponding to the IGRF values at the centre of the study region.

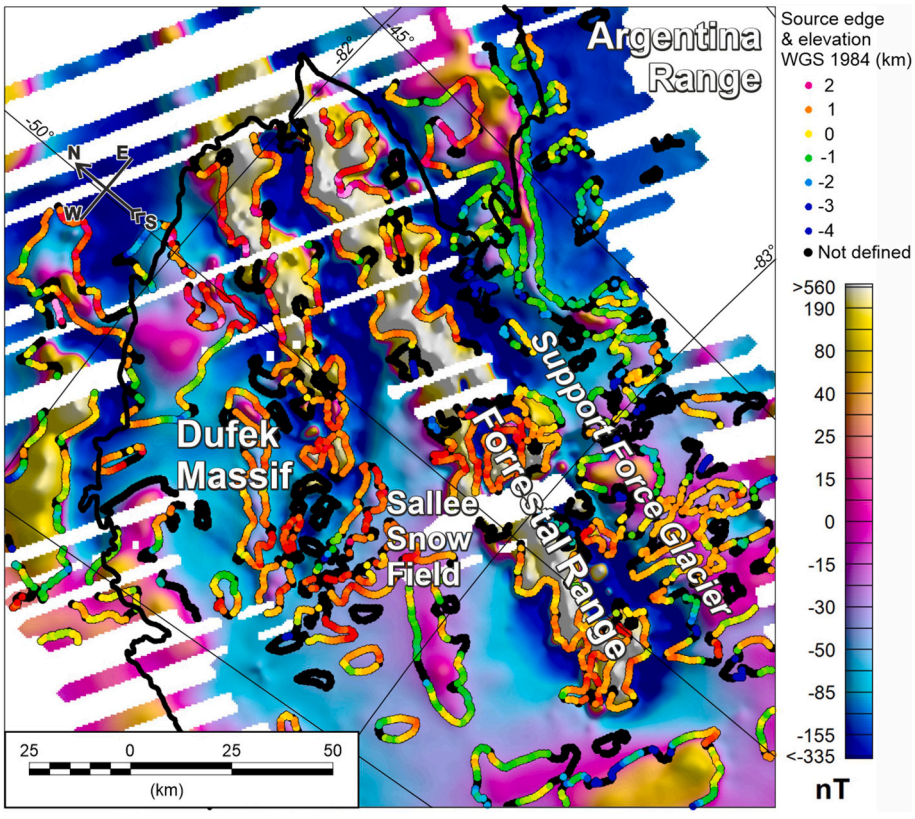

Fig. 4. Elevation of magnetic sources from the tilt depth method. Note many sources appear to be above sea-level, consistent with the elevated and highly magnetic topography in the region.

3. Results

3.1. Compiled magnetic anomaly map

Our new magnetic compilation clearly identifies the signature of the two previously reported branches of the Dufek Intrusion (Fig. 3). The highest amplitude magnetic anomalies are in the Eastern branch (Forrestal Range), where peak anomaly amplitudes of 2600 nT are observed, with many other areas having amplitudes between 500 and 1000 nT. The Western branch also shows multiple broad anomalies with amplitudes of 500 to 1000 nT, but these are restricted to the snow-covered northern part. The outcropping rocks in the Dufek Massif are generally associated with lower amplitude magnetic anomalies between 80 and 600 nT, aside from a single isolated and spatially restricted 1000 nT anomaly. The trend of the anomalies in the Dufek Massif follows the topographic trend (Fig. 3b), which is offset from the trend of the higher amplitude parts of the western and eastern branches of the intrusion.

In addition to the two main magnetic structures previously reported, higher resolution data (2.5 km line spacing) over the Support Force Glacier reveals a distinctive magnetic anomaly at least 70 km long and 4–10 km wide, with a typical amplitude of ~140 nT (Fig. 3b). This Support Force Anomaly runs in a straight line ~50 km south-west from the coast, before abruptly turning southeast and out of the survey area. The anomaly appears to continue in a more diffuse form north of the coast, but this may be an artifact of the altitude, line spacing and reduced navigational accuracy of previous surveys.

Beneath, and to the south of the Sallee Snow Field there is a further approximately linear magnetic anomaly with an amplitude of ~30 nT (Fig. 3a). This anomaly has previously been linked with one of a number of Jurassic dykes originating in the Forrestal Range (Ferris et al., 2003). However, due to the relatively wide line spacing of the underlying survey (5 km), compared to the Support Force Survey (2.5 km), the anomaly is relatively hard to trace, and it is not clear if it originates in the Dufek Massif or Forrestal Range. The relatively low amplitude and indistinct nature of the anomaly compared to other parts of the intrusive system mean we do not model this feature.

Other magnetic anomalies are present south and west of the exposures of the Dufek Intrusion. These typically have amplitudes of <100 nT, and have previously been attributed to Cambrian igneous rocks associated with the ~500 Ma orogenic event in this region (Ferris et al., 1998; Ferris et al., 2003). The likely source rocks for these anomalies are the pre-Jurassic igneous rocks (Fig. 2a) which show relatively elevated susceptibility and are exposed in the southern Pensacola Mountains (Storey et al., 1996) (Fig. 2b). A similar broad low amplitude magnetic anomaly with no strong preferred orientation is noted over the southern end of the Support Force Glacier (Fig. 2a). The source for this anomaly is not clear, but it appears distinct from both the high amplitude anomalies over the Forrestal Range, and the linear structure to the north, and we therefore attribute it to magnetic basement.

In the Forrestal Range the edges of the anomaly sources indicated by the TDX enhancement are broadly consistent with the boundary between outcropping gabbros and surrounding outcrops of less magnetic sediments (Fig. 3c). In contrast, in the Dufek Massif area outcrops of gabbro appear to be outside main source body indicated by higher amplitude magnetic anomalies and the TDX edge enhancement, however, these outcrops are within the broader negative total field anomaly and are associated with local source body margins in the TDX enhancement.

Depth to magnetic source estimation using the tilt depth method confirms the sources for the Dufek and Forrestal bodies are generally very shallow, in line with the presence of exposed high magnetic susceptibility rocks. However, we note that 75 % of the recovered sources are shallower than the bed. This suggests that there is a systematic bias in the depth to source results which we attribute this to limitations imposed by the assumptions behind the tilt depth method, including the sources being simple vertical contacts and no remnant magnetisation being present. Despite this we believe that the conclusion that sources are generally shallow is valid.

3.2. Gravity anomaly compilation

The free air gravity anomalies show positive values associated with the topography of the Forrestal Range and a broad negative over the adjacent deep basin of the Support Force Glacier (Fig. 5a). The Bouger gravity anomaly retains a relative positive anomaly over the Forrestal range, ~70 mGal above the adjacent values (Fig. 5b). The Bouguer anomalies over the more elevated topography west of the Forrestal range are between −70 and − 55 mGal, while to the east values of −55 to −45 mGal are observed. The Airy isostatic anomaly, which has been corrected for the theoretical crustal thickness variations required to balance the observed surface topography, retains the ~70 mGal relative positive over the Forrestal range, while the anomalies to the east over the Support Force Glacier are more negative than those to the west (Fig. 5c). A good visual correlation between the outcrop of the Dufek Intrusion and the local residual positive Airy isostatic gravity anomaly is seen (Fig. 5c).

The regional view of the Airy isostatic anomaly (Fig. 5d) includes land gravity observations over both the Forrestal Range and Dufek Massif. These show values 50 to 100 mGal above the regional background. In the case of the Dufek Massif background gravity values away from the rock outcrops are not sampled, but it is likely that the values recorded in the Dufek Massif reflect a significant local positive relative gravity anomaly. This is consistent with the positive anomalies seen in the Operation Ice Bridge data to the north of the region. A broad correlation is seen between the Sallee Snow Field magnetic anomaly (Fig. 3c) and a ~ 10 mGal relative gravity high (Fig. 5d). However, the lack of short wavelength resolution in the gravity field due to data processing and low amplitude relative to the error of the gravity anomalies mean this feature is poorly resolved and hard to interpret.

3.3. 3D model outputs

The joint gravity and magnetic 3D forward model of the southern Forrestal Range was able to reproduce the general form and amplitude of the observed anomalies (Figs. 6 and 7). The overall misfit between observed and modelled gravity anomalies had a standard deviation of 10 mGal, while the magnetic data showed a misfit of 150 nT. While these errors are high, the aim was not to fit the data perfectly, but rather to explore the possible form of the intrusion which gave a visually acceptable fit to both gravity and magnetic data. Assuming a modelled density of 3000 kgm^{-3} (330 kgm^{-3} above the model background) in line with values measured for gabbros across the Forrestal and Dufek Ranges (Ford and Nelson, 1972), the gravity data required a source body 5 to 7 km thick. A thicker source would only be permissible, from a gravity perspective, if the intrusion had a significantly lower density, or if the surrounding rocks had higher density. However, observations indicate that while there is scatter in the measured density, the density weighted for the typical intrusive rock-types remains close to 3000 kgm^{-3} (Ford and Nelson, 1972). In addition, outcropping rocks show the intrusion is emplaced within a sequence of meta-sedimentary units, which likely conform to an average crustal density of approximately 2670 kgm^{-3}, with higher background densities therefore unlikely.

It was not possible to closely match the magnetic anomalies assuming a single susceptibility for the entire presumed intrusive body required by the gravity data. To match the high amplitude and relatively short wavelength of the magnetic anomalies shallow and high susceptibility (10,000 × 10^{-5} SI) material was required. We then assumed the deeper parts of the intrusion indicated by the gravity data had a lower, but not insignificant susceptibility of 1000 × 10^{-5} SI. The highest susceptibility values are in line with measurements of samples of the Saratoga Gabbro, which forms much of the outcrop in the Forrestal Range (Fig. 2), while the lower values could be consistent with either the

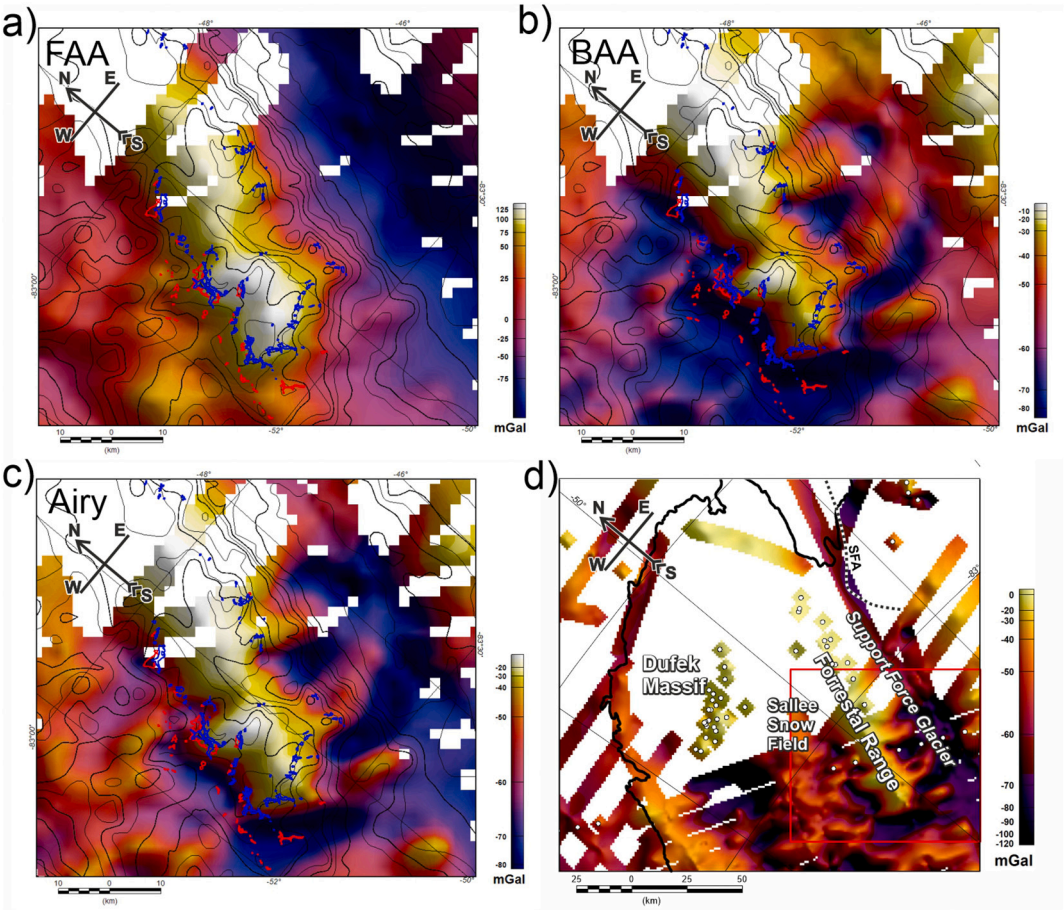

Fig. 5. Gravity anomaly maps. a) Airborne free air gravity anomaly map (Jones, 2020; Tinto et al., 2010, updated 2019). Contours show elevation from Bedmachine V2 (Morlighem et al., 2020). Blue lines mark outcropping Jurassic magmatic rocks. Red lines mark surrounding rocks, location red box in (d). b) Bouger gravity anomaly. c) Airy Isostatic residual gravity anomaly. d) Wider map of Airy isostatic gravity anomalies. Circles show locations of point land gravity data (Behrendt et al., 1974). Also note regional Operation Ice Bridge flight lines. Red box locates (a–c). Dashed line marked SFA marks magnetic Support Force Anomaly. (For interpretation of the references to colour in this figure legend, the reader is referred to the web version of this article.)

Saratoga or Aughenbaugh Gabbro. Assuming deeper parts of the intrusion have lower susceptibility is in-line with the previous geological assumption that the lower susceptibility Aughenbaugh Gabbro exposed in the Dufek Massif forms the lower part of the intrusion (Fig. 2).

It is apparent from the 2D profiles that it is not always possible to match the peaks of the magnetic and gravity anomalies associated with the intrusion, while maintaining the two chosen susceptibility values and the high density for the intrusive body (Fig. 7). This indicates that local complexity, including rocks with extremely high magnetic susceptibility and/or strong remnant magnetisation are present within the Forrestal Range. It is also apparent that the peaks in the magnetic anomalies are often offset to the west of the peak in the Airy isostatic gravity anomaly. Our model therefore has the deeper lower susceptibility rocks offset to the east. Although a subtle signal, this offset was required on all joint gravity/magnetic modelled profiles. There is no evidence of major positive gravity anomalies co-occurring with magnetic anomalies west of the main Forrestal Range (Fig. 5c). The modelled eastward dip of the western edge of the Forrestal Range is consistent with that seen in outcrop where the contact was noted to dip ~45° to the southeast (Semenov et al., 2014).

Our 3D magnetic model for the wider Dufek Intrusion (Fig. 8) used the initial thickness and susceptibility values from the local combined gravity and magnetic model as a starting point. The detailed amplitude of every magnetic anomaly could not be matched by our simplified model, but the overall form and amplitude of the main magnetic anomalies in this region are reproduced (Fig. 8). The highest-susceptibility parts of the intrusion are confined to the north and east of the modelled structure, where in places the model required that almost the entire body was high susceptibility material. In some places our forward model placed material above the ice sheet bed, in an aim to match the observed anomaly (Fig. 9a). This indicates that either the bed elevation is incorrect, or the source has a particularly high susceptibility in this region. In contrast, the Dufek Massif, which is associated with lower amplitude anomalies, required a reduction in the maximum modelled susceptibility to 5000×10^{-5} SI and is dominated by even lower susceptibility material (Fig. 9b), consistent with the lower measured susceptibility from samples of the Aughenbaugh Gabbro. It is also noted that no magnetic material is required in our model between the exposures of the Dufek Massif and Forrestal Range. Across our wider magnetic model we maintain a basal depth of 5 km, as we have no direct evidence of a significantly thicker or thinner structure.

In addition to the two main branches of the intrusion we also model a lower amplitude anomaly with a linear body east of the main intrusion, located in the region of the Support Force Glacier. As there is no information about the susceptibility of this body we arbitrarily used a value of 4000×10^{-5} SI, consistent with some of the lower values measured in the adjacent Saratoga Gabbro (Fig. 2). With this susceptibility, the amplitude and wavelength of the observed anomaly could be matched by a source body ~1 km thick and 5 km wide, assuming the body was at or close to the ice-bed interface, as suggested by the depth to source estimates (Fig. 4). If the body was dominated by a lithology equivalent to the Lexington Granophyre, which is assumed to form the stratigraphic

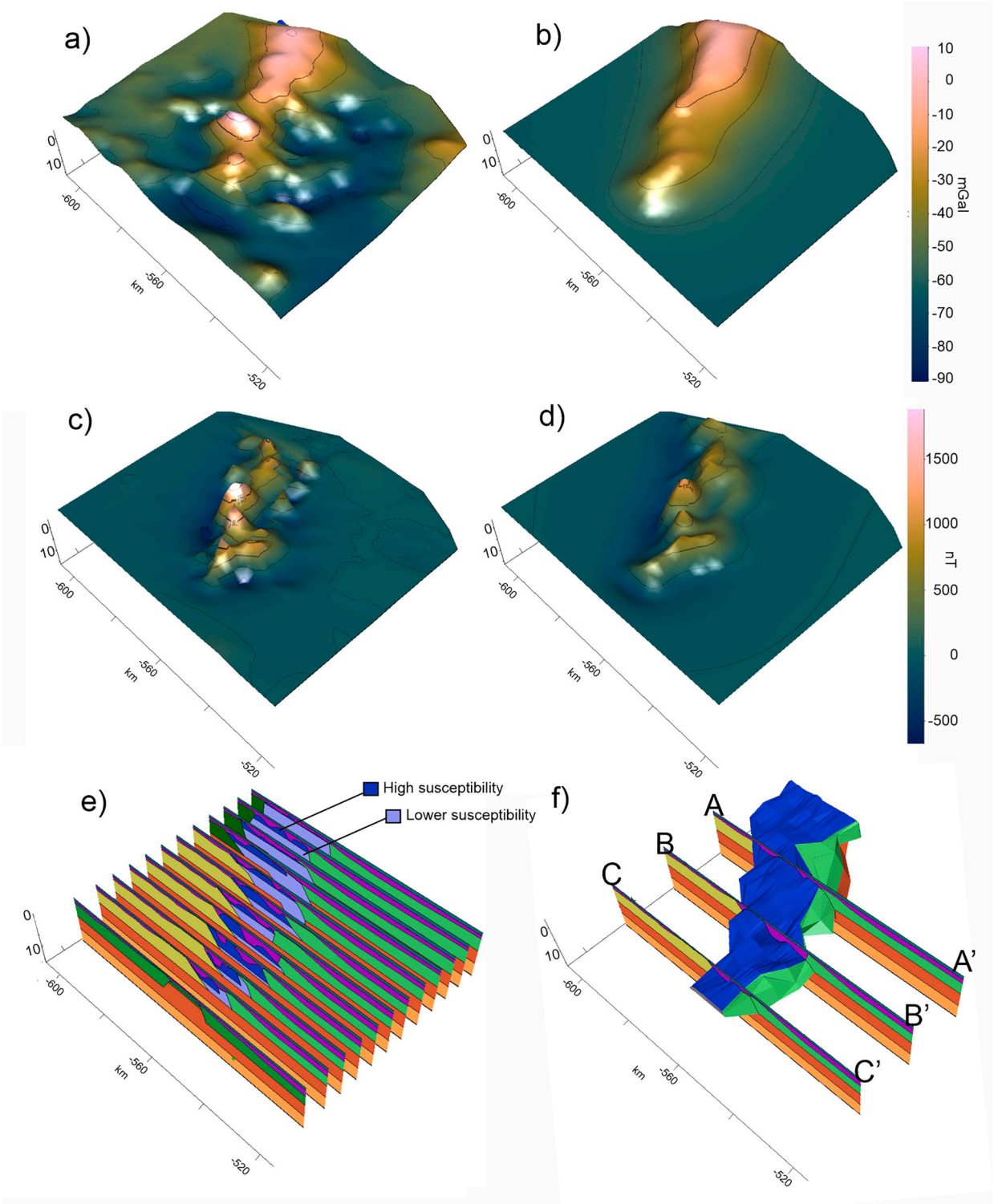

Fig. 6. Results of joint 3D forward gravity and magnetic model using iGMAS+ software. Viewed looking from the southeast to the northwest. Coordinates are projected polar stereographic km aligned with the other maps in the paper. a) Observed Airy isostatic gravity anomaly. b) Modelled gravity anomaly. c) Observed magnetic total field anomaly. d) Modelled magnetic total field anomaly. e) 2D sections used to construct model. Note all rocks were assumed to have zero susceptibility and density contrast aside from the indicated high and lower susceptibility bodies. f) 3D shape of modelled intrusive body, with three selected sections (A, B and C) shown in Fig. 7 highlighted.

cap to the wider intrusion, an even lower susceptibility may be appropriate (~1500 × 10^{-5} SI, Table 1). However, this would require a source body between three and five km thick, which is large compared to the thickness of similar caping rocks in other large intrusions such as the Bushveld (VanTongeren et al., 2016).

Our 3D modelling provides a preliminary estimate of the volume of magma emplaced within the two main lobes of the Dufek Intrusion and the Support Force body, shown in Fig. 8d, of ~23,715 km^3. If the volume between the Dufek Massif and Forrestal Range bodies was occupied by intrusive material, the total volume would increase by ~38 % to 32,814

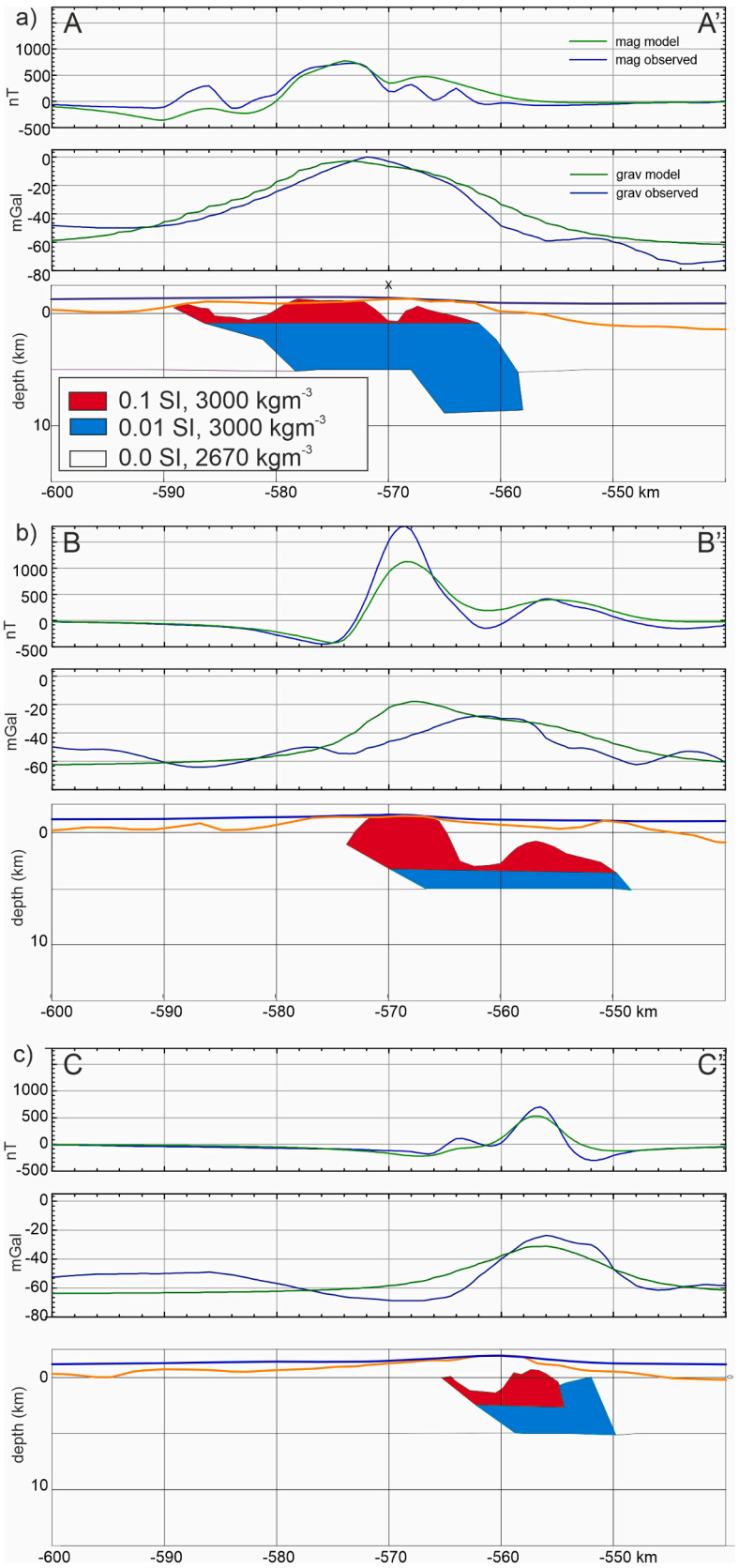

Fig. 7. Selected 2D sections used to construct the 3D model, see Fig. 6f for location. a) is grid north, b) central and c) southern. Upper panels show magnetic data and model, central panels show gravity data and model. Lower panels show modelled crustal structure. Note shallower high susceptibility body offset west of the deeper part of the modelled intrusion.

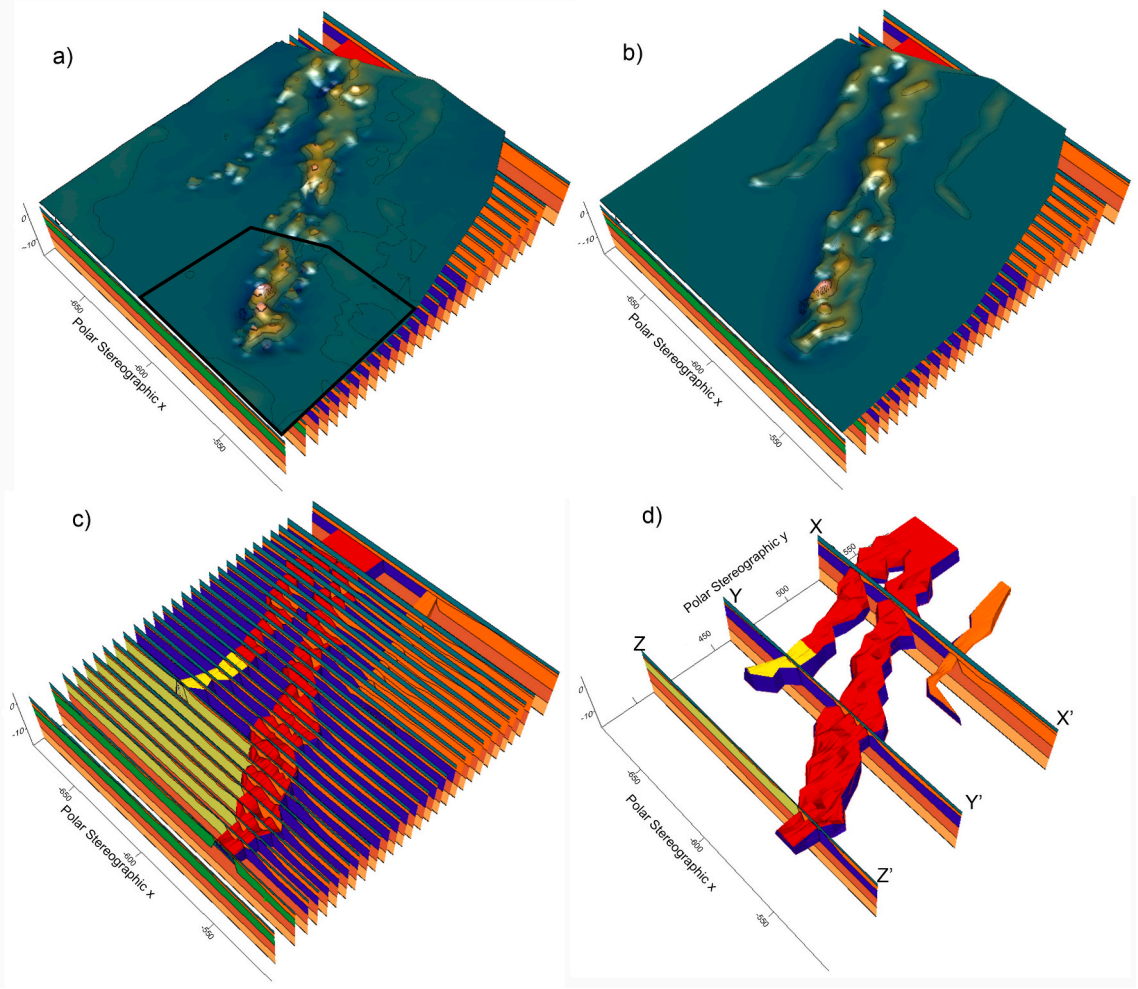

Fig. 8. 3D magnetic only forward model of the wider Dufek Intrusion. a) Input magnetic data. Black outline locates joint magnetic and gravity model (Fig. 6). b) Modelled magnetic anomaly. c) 2D sections used to construct forward model. d) 3D volume of rocks with imposed magnetic susceptibility. All other rocks in the model volume are assumed to have zero susceptibility. Three sections (X, Y and Z) locate selected 2D profiles shown in Fig. 9.

km^3. However, there is no requirement in the model, or from other geophysical observations, for this infilling and we therefore prefer the lobe model as discussed further in Section 4. Within the modelled main two lobed intrusion ~9685 km^3 of material (~41 %) forms the upper high susceptibility layer, while the lower susceptibility material modelled to make up the lower part of the intrusion and the exposed Dufek Massif has a volume of ~13,483 km^3 forming ~57 % of the intrusion. The Support Force body has a volume of ~546 km^3, accounting for ~2 % of the total volume, assuming a susceptibility of 4000 $\times$ 10^{-5} SI. Given the acknowledged uncertainty in our visual fit of the model to data the total thickness of the intrusion which is modelled to be ~6 km, could be between 9 and 3 km. This equates to an uncertainty in the volume calculation of ±12,000 km^3. Even given the large uncertainty, this makes the Dufek Intrusion larger by volume than the Great Dyke (10,931 km^3) calculated from published area and thickness estimates (Chaumba, 2022) and approximately equivalent in volume to the ~24,700 km^3 Stillwater complex, calculated from geophysical modelling (Finn et al., 2020).

4. Discussion

Two end members for the structure of the Dufek Intrusion have been proposed. First a simple single box-like intrusion linking all outcrops, which differentiated and solidified before being tilted to the east e.g. (Ford, 1976; Semenov et al., 2014). Alternatively, the intrusion may be a complex superposition of distinct magmatic events, offset by numerous fault systems (Ferris et al., 1998). Our new data compilation and 3D models help to distinguish these endmembers.

The localised Airy isostatic gravity and anomaly (Fig. 4c) and 3D modelling of the gravity dataset (Figs. 6, 7) give no indication of a dense body extending west of the Forrestal Range. Therefore, at least in the southernmost area, the outcrops in the Dufek Masif and Forrestal Range are not directly linked in an E/W direction. This is consistent with the outcrop of sedimentary rocks east of the Forrestal Range and the steeply southeasterly dipping contact of the intrusion exposed at Mount Lechner. The separation between the branches of the intrusion is supported by the TDX enhancement of the magnetic anomaly margins (Fig. 3b), and forward models of the magnetic field (Figs. 8 and 9) which do not indicate or require any E/W link between the outcrops, or between the eastern and western branches of the intrusion, aside from in the very far north. The modelled eastward offset of the thick but lower susceptibility part of the intrusion in the Forrestal Range, compared to the highest susceptibility material, also supports a more complex structural model (Fig. 10a). In the simple box case (Fig. 10b), assuming magnetic susceptibility increases upward within the intrusion, the thickest part of the intrusion in the east should directly correspond with the thickest section of highly magnetic material, which is not seen. We therefore do not favour a model where the Dufek Intrusion is a single tilted block, (Ford, 1976; Semenov et al., 2014) favouring instead, two distinct main lobes, akin to (Ferris et al., 1998).

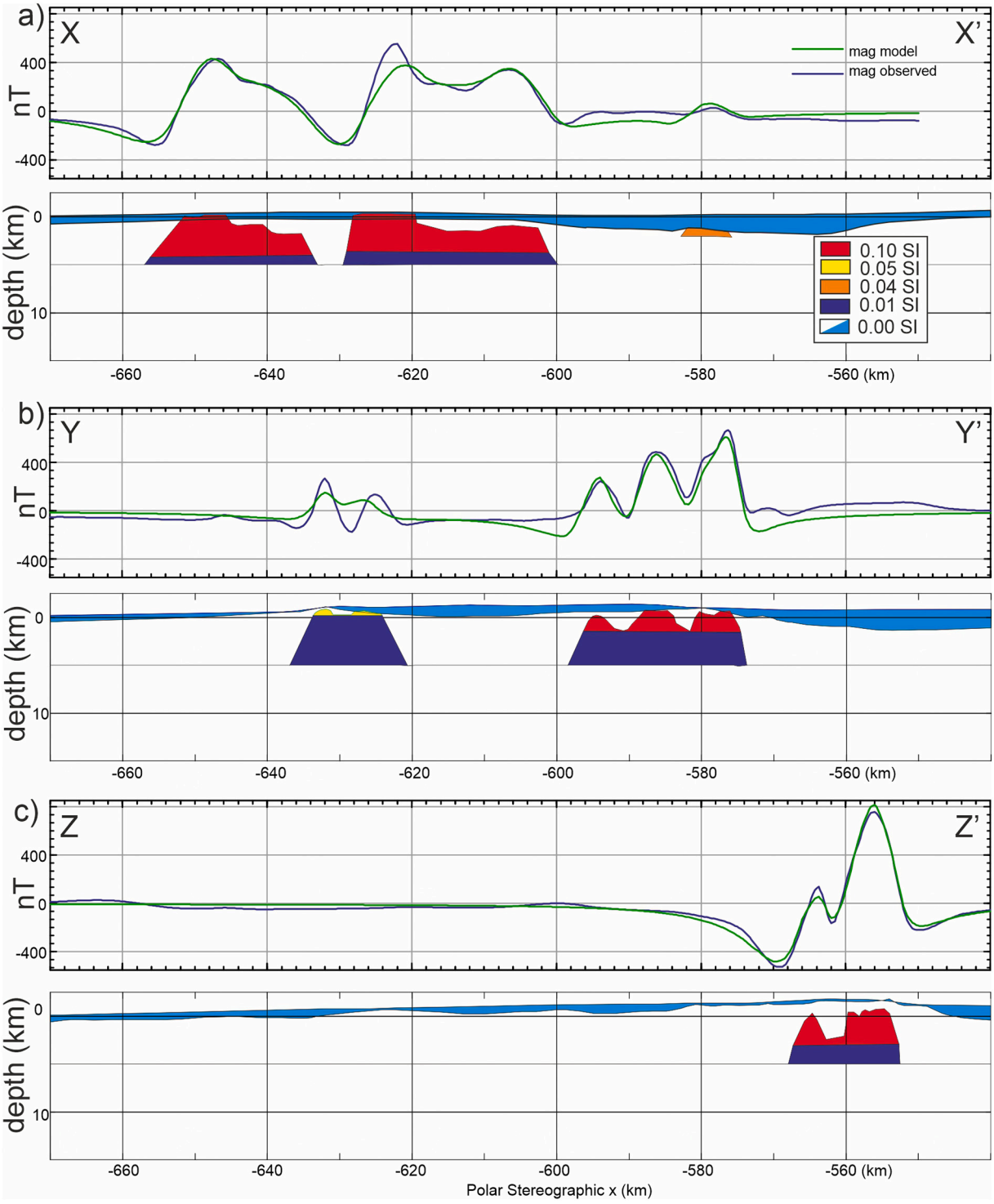

Fig. 9. Selected 2D models used in the construction of the wider 3D magnetic only model. a) Northern model including Eastern and Western branches, and Support Force Glacier intrusion. Note no outcrop constrains this profile. b) Central model over exposed section of Dufek Masif and Forrestal Range. c) Profile only intersecting Forrestal Range outcrops.

Although 3D models favour distinct eastern and western branches of the main intrusive structure, both branches can be modelled with a similar higher susceptibility upper layer, consistent with the Saratoga Gabbro, overlaying a lower susceptibility layer (Fig. 10c and d). This double layered structure is required to provide an adequate fit to the joint magnetic and gravity model, using realistic susceptibility and density values (Figs. 6 and 7). We make the simplifying assumption that this two-layer model extends to all regions requiring extremely high susceptibility to fit the observed anomalies. This is supported by land gravity data which shows the Dufek Massif is associated with positive gravity anomalies of a similar magnitude to the Forrestal Range, consistent with a layer of dense material of similar thickness to that modelled in the Forrestal Range (Fig. 10a). Previous authors have suggested a thickness of 6.2–8.8 km for the overall intrusion based on this land gravity data (Behrendt et al., 1974), in line with our model results. If the simpler box model was correct the Forrestal Range should be

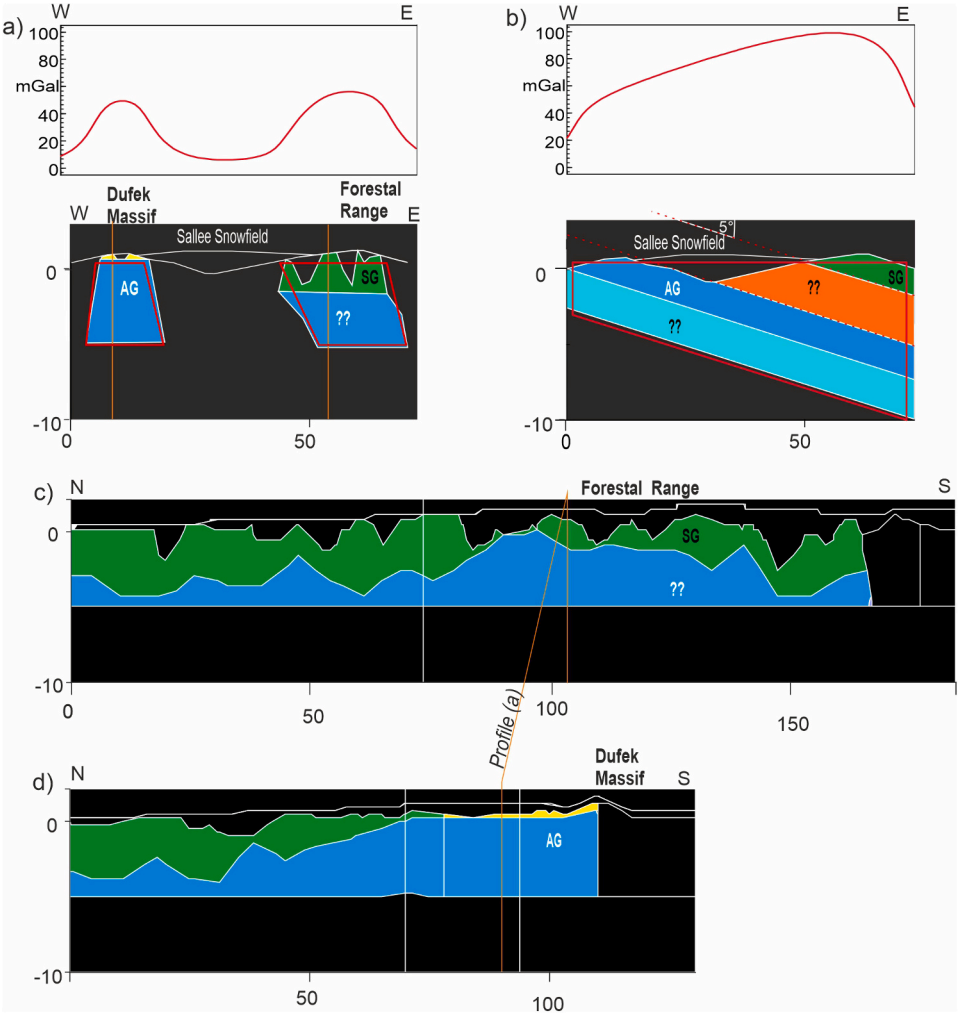

Fig. 10. Intersecting slices of 3D intrusion model located on Fig. 3b. a) EW section of model between outcrop in the Dufek Massif and Forrestal Range. Upper panel shows results of simplified two body gravity model. Lower panel shows crustal section. Red lines show bodies used in simple gravity model, coloured bodies from 3D magnetic model. Orange lines mark intersections with longitudinal profiles. b) Alternative hypothesis for a simple tilted box intrusion on the same profile as (a) (Ford, 1976; Semenov et al., 2014). Upper panel shows result of simplified gravity model (red body in lower panel). Note amplitude of gravity anomaly in Forrestal Range is almost double that in the Dufek Massif. c) Longitudinal section of the model of the Eastern branch of the intrusion. d) Longitudinal section of the model following the western branch of the intrusion. (For interpretation of the references to colour in this figure legend, the reader is referred to the web version of this article.)

underlain by almost twice as much dense material and simple 2D modelling shows the positive gravity anomalies in the Forrestal Range would be twice as large (Fig. 10b).

The highest susceptibility layer is not required in the Dufek Massif, where material with susceptibility consistent with the exposed Aughenbaugh Gabbro can be used to model the observed anomalies. Although the amplitude and strike of the magnetic anomaly changes between the Dufek Massif and the ice covered part of the intrusion further to the north (Ferris et al., 1998), there is no distinct break indicated by our calculated TDX enhancement (Fig. 3b). Therefore, in contrast to Ferris et al. (1998), we interpret the rocks exposed in the Dufek Massif as part of the same intrusive complex as the buried material further north. Although the line spacing is sparse, it appears that the eastern and western branches of the high amplitude anomaly do merge into a single feature just north of the coastline, consistent with the entire Dufek Intrusion, including both the Dufek and Forrestal branches, being a unified magmatic structure. This is supported by dating evidence which indicates that rocks of the Dufek and Forrestal branches crystalised within ~160 ka of each other (VanTongeren et al., 2020), suggesting the intrusion developed within a single overarching magmatic event.

Our model shows that the magnetic and gravity anomalies across the Dufek Massif and Forrestal Range can be created by a single mafic intrusive body (the Dufek Intrusion), consisting of two distinct lobes. Our modelling of the existing data supports the hypothesis that the intrusion is vertically stratified, with higher susceptibility at shallower levels. Our simplified model assumes two layers, but in reality, the intrusion is likely to show a much more complex multi-layered structure, but showing an overall increase in susceptibility upwards. The presence of a more complex structure and localised very high susceptibility is indicated by the extremely high amplitude magnetic anomalies, which can't be matched by our forward model which limits the maximum susceptibility.

An additional structure east of the Forrestal Range, beneath the Support Force Glacier (Figs. 3 and 8) is also indicated by our data and modelling. Previously, the northern end of this anomaly was interpreted as a basement block translated from Berkner Island (Ferris et al., 1998). However, our updated compilation shows that this anomaly continues southward as a narrow (~5 km wide) linear structure, which turns abruptly from a N/S trend to a NW/SE trend. Such a pattern is inconsistent with a basement block, and we therefore interpret this structure as an intrusive magmatic body. The structure shares the same trend as Forrestal Range anomalies, suggesting it formed during the same phase of magmatism (Fig. 3b). Additional dyke-like structures associated with the Dufek Intrusion are expected, given the significant extent of the

Ferrar dolerite sills which are thought to be a shallow part of the same intrusive system. Such dykes have previously been interpreted beneath the Sallee Snow Field based on magnetic data (Ferris et al., 2003), although they are not modelled in this study as they are relatively indistinct in our compilation (Fig. 3a).

The proposed Support Force Intrusion is similar in width (4–10 km) to the Archean Great Dyke of Zimbabwe, which is a strongly linear layered mafic intrusion, that also presents a significant linear positive magnetic anomaly (Ranganai et al., 2016). Although a link with the Dufek Intrusion is likely, with available data it is not possible to prove definitively and the structure may reflect a pre-Jurassic, or a more recent magmatic event, following the same regional Cambrian structural grain exposed in the Pensacola Mountains. Further higher resolution aeromagnetic data to the north of the study area is required to resolve any linkage.

The linear shape of the structures forming the Dufek Intrusion and adjacent Support Force Intrusion indicate magmatic emplacement was structurally controlled. The underlying deformed Ross age metasediments seen in the southern Pensacola Mountains broadly share the same ~N/S structural grain as the Forrestal Range, suggesting this is the dominant structural control. However, the Dufek Massif shows a switch to a NNE/SSW trend, which is approximately parallel to the Jurassic Pagano Shear Zone separating East Antarctica from the provinces of West Antarctica which were tectonically active more recently (Jordan et al., 2013). The Pagano Shear Zone is thought to have accommodated ~500 km of strike slip motion and is dated to ~178 Ma by an elongated granite emplaced within it (Jordan et al., 2013), however, the correspondence with the strike of the Dufek Massif part of the intrusion suggests this structural grain, and potentially the Pagano Shear Zone itself, was present at ~182 Ma. In contrast to the Dufek Massif region the Support Force Intrusion shows a N/S trend with a turn to the NW/SE, indicating magma further inboard within East Antarctica was experiencing a different pattern of structural control and/or structural inheritance.

Layered intrusions in other regions globally are interpreted to have been fed from deep-seated magma sources, exploiting crustal weaknesses, before spreading laterally in the upper crust. Such feeder zones are typically imaged by gravity data, for example in the Bushveld Complex three potential feeders >15 km deep formed of dense, but relatively low magnetic susceptibility material, are modelled (Cole et al., 2021). In the Bushveld Complex, such feeders are sourced from deep magmatic staging chambers, which are intersected by major crustal scale faults, providing pathways for magma flow to shallow levels (Cole et al., 2024). This is similar to the Mesoproterozoic Duluth Complex, a major component of the US Midcontinent Rift System, where feeders extending to >20 km depth and bounded by a major fault system are recognised (Peterson et al., 2023). Gravity data over the Great Dyke in Zimbabwe also indicates a central feeder zone extending to depths of 6 to 10 km, giving the intrusion a trumpet-shaped form (Wilson, 1996). Within our datasets and models the lack of comprehensive gravity data coverage means we cannot provide definitive evidence for a feeder zone. The modelled thickening of the Forrestal part of the intrusion (Fig. 7a) could point to this type of structure. However, as the Dufek Massif and Forrestal Range branches appear to merge into a single magnetic feature in the north it is proposed that this is the most likely location of the main conduit to the deeper magmatic system. This location is also proximal to the Pagano Shear Zone (Fig. 1), a major crustal fault system which may have facilitated magma flow towards the surface. We propose that magma reaching mid to upper crustal levels along the Pagano Shear Zone then likely intruded to the south, forming the observed main two-lobed structure and smaller associated dykes.

The distinct susceptibility indicated by our models for the upper and lower parts of the intrusion could reflect either fractional crystallisation of a single magmatic pulse, or multiple phases of magmatic emplacement, within a broader magmatic event. We favour the latter hypothesis as longitudinal profiles through the model of the intrusion show the Aughenbaugh Gabbro of the Dufek Massif lies beside, as well as beneath the higher susceptibility material to the north, rather than presenting a simple vertically layered structure (Fig. 10c and d). Dating evidence also suggests that, although close in age, the rocks of the Dufek Massif are slightly younger, crystallising ~160 ka after those in the Forrestal range (VanTongeren et al., 2020). This appears to contradict the suggestion that the higher susceptibility rocks formed from crystallisation of a later stage residual melt, as the lower susceptibility part crystalised later. The formation of layered intrusions through interaction of multiple intrusive phases in the same location, rather than simple solidification of a single large intrusion, is also becoming accepted following more detailed studies of other large intrusions such as the Bushveld Complex (Scoates et al., 2021). An alternative model where the difference in zircon age is associated with the slow rate of cooling of a single large body, meaning the zircon saturation temperature was reached later deeper within the large intrusion, is also a possibility.

5. Conclusions

Digital enhancement and 3D modelling of magnetic and gravity data suggest that the Jurassic Dufek Intrusion in Antarctica has a volume of ~23,000 km^{-3} making it amongst the largest in the world, but smaller than the Bushveld Intrusion of southern Africa. It is composed of two main lobes, 120 to 180 km long, with no geophysical evidence of cross linking, aside from in the very far north.

Modelling suggests over 50 % of the intrusion is formed of a lithology with a susceptibility consistent with outcrops in the Dufek Massif, while ~40 % of the intrusion is formed by rocks with anomalously high susceptibility consistent with those rocks exposed in the Forrestal Range. The similarity between the two lobes in our 3D model, and lack of distinct offset in magnetic signatures between the Dufek Massif and areas to the north, leads us to prefer a model where both lobes were created by the same overarching magmatic event. However, the difference in modelled susceptibility and the geometry of this variability leads us to suggest that at least two pulses of magmatism with differing geochemistry occurred, consistent with contrasting dates for different parts of the intrusion.

We identify an additional adjacent ~70 km long linear magnetic feature, modelled to be a body 1–2 km thick and 4–5 km wide, which may form part of the same magmatic system, but is now buried beneath the Support Force Glacier. This approximately parallel structure is of a similar width to the Great Dyke within the Zimbabwe Craton (Ranganai et al., 2016), and may reflect a feeder for the wider Ferrar magmatic province. Tracing this structure to the north and southeast with future high resolution aerogeophysical surveys would help confirm if this is a Jurassic structure, and if so, did it act as a feeder linking the Dufek Intrusion to the wider Ferrar magmatic system.

CRediT authorship contribution statement

Tom A. Jordan: Writing – original draft, Visualization, Methodology, Formal analysis, Conceptualization. **Teal R. Riley:** Writing – review & editing, Conceptualization.

Declaration of competing interest

The authors declare that they have no known competing financial interests or personal relationships that could have appeared to influence the work reported in this paper.

Data availability

Data used in this publication is avaialble from the UK Polar Data Centre, or other data repositories, with citations provided in the text

Acknowledgements

This work is supported by the NERC National Capability - Polar Expertise Supporting UK Research (NCSS) programme. This study includes data provided by the Polar Rock Repository with support from the National Science Foundation, under Award OPP-2137467. We also thank the Filchner Ice Shelf System (FISS) project for collecting the new opportunistic aeromagnetic data set.

References

Anikiev, D., Götze, H.-J., Meeßen, C., Plonka, C., Scheck-Wenderoth, M., Schmidt, S., 2020. IGMAS+: Interactive Gravity and Magnetic Application System, vol. 1.3. GFZ Data Services.

Beck, M.E., 1972. Palaeomagnetism and magnetic polarity zones in the Jurassic Dufek intrusion, Pensacola Mountains, Antarctica. Geophys. J. Int. 28, 49–63.

Behrendt, J.C., Henderson, J.R., Meister, L., Rambo, W.L., 1974. Geophysical Investigations of the Pensacola Mountains and Adjacent Glacierized Areas of Antarctica.

Behrendt, J.C., Drewry, D.J., Jankowski, E.J., Grim, M.S., 1980. Aeromagnetic and radio echo ice-sounding measurements show much greater area of the Dufek Intrusion, Antarctica. Science 209, 1014–1017. https://doi.org/10.1126/science.1209.4460.1014.

Burgess, S.D., Bowring, S.A., Fleming, T.H., Elliot, D.H., 2015. High-precision geochronology links the Ferrar large igneous province with early-Jurassic ocean anoxia and biotic crisis. Earth Planet. Sci. Lett. 415, 90–99.

Carnes, J.D., Cheadle, M.J., Gee, J.S., Grimes, C.B., Swapp, S.M., 2011. The magmatic and thermal history of the Dufek Complex, Antarctica. Eos, Trans. Am. Geophys. Union Fall Meeting 2011, V33C–2661.

Cawood, P.A., 2005. Terra Australis Orogen: Rodinia breakup and development of the Pacific and Iapetus margins of Gondwana during the Neoproterozoic and Paleozoic. Earth Sci. Rev. 69, 249–279.

Chaumba, J.B., 2022. A review of the emplacement and formation of magmatic platinum-group elements-enriched deposits in large layered mafic/ultramafic intrusions, with special reference to the "big three" (Stillwater Complex, Great Dyke, and Bushveld Complex). J. Afr. Earth Sci. 194, 104603.

Cole, J., Finn, C.A., Webb, S.J., 2021. Geometry of the Bushveld Complex from 3D potential field modelling. Precambrian Res. 359, 106219.

Cole, J., Finn, C.A., Jane Webb, S., 2024. Deep magmatic staging chambers for crustal layered mafic intrusions: an example from the Bushveld Complex of southern Africa. Precambrian Res. 403, 107306.

Cooper, G.R.J., Cowan, D.R., 2006. Enhancing potential field data using filters based on the local phase. Comput. Geosci. 32, 1585–1591.

Cox, S.C., Smith Lyttle, B., Elkind, S., Smith Siddoway, C.S., Morin, P., Capponi, G., Abu-Alam, T., Ballinger, M., Bamber, L., Kitchener, B., Lelli, L., Mawson, J.F., Millikin, A., Dal Seno, N., Whitburn, L., White, T., Burton-Johnson, A., Crispini, L., Elliot, D., Elvevold, S., Goodge, J.W., Halpin, J.A., Jacobs, J., Mikhalsky, E., Martin, A.P., Morgan, F., Smellie, J., Scadden, P., Wilson, G.S., 2023. The GeoMAP (v.2022-08) continent-wide detailed geological dataset of Antarctica. PANGAEA. https://doi.org/10.1594/PANGAEA.951482.

Curtis, M.L., 2002. Palaeozoic to Mesozoic polyphase deformation of the Patuxent Range, Pensacola Mountains, Antarctica. Antarct. Sci. 14, 175–183.

Curtis, M.L., Millar, I.L., Storey, B.C., Fanning, M., 2004. Structural and geochronological constraints of early Ross orogenic deformation in the Pensacola Mountains, Antarctica. Geol. Soc. Am. Bull. 116, 619–636. https://doi.org/10.1130/B25170.25171.

Dunlop, M., Cheadle, M., Grimes, C., Swapp, S., Scott, S., Gee, J., 2016. The Dufek Complex: Growth by periodic replenishment in one of the World's largest layered mafic intrusions. In: GSA Annual Meeting Geological Society of America, Denver, Colorado, USA - 2016.

Ferris, J.K., Johnson, A.C., Storey, B.C., 1998. Form and extent of the Dufek intrusion, Antarctica, from newly compiled aeromagnetic data. Earth Planet. Sci. Lett. 154, 185–202.

Ferris, J.K., Storey, B.C., Vaughan, A.P.M., Kyle, P.R., Jones, P.C., 2003. The Dufek and Forrestal intrusions, Antarctica: a centre for Ferrar Large Igneous Province dike emplacement? Geophys. Res. Lett. 30. https://doi.org/10.1029/2002GL016719.

Finn, C.A., Zientek, M.L., Parks, H.L., Peterson, D.E., 2020. Mapping the 3D extent of the Stillwater Complex, Montana—implications for potential platinum group element exploration and development. Precambrian Res. 348, 105860.

Ford, A.B., 1976. Stratigraphy of the Layered Gabbroic Dufek Intrusion, Antarctica, Bulletin 1405-D.

Ford, A.B., Nelson, S.W., 1972. Density of the stratiform Dufek intrusion, Pensacola Mountains, Antarctica. Antarct. J. U.S. 7, 147–149.

Gee, J., Lusk, M., Cheadle, M., Grimes, C., Meurer, W., 2009. Origin and Significance of Magnetic Anisotropy in the Dufek Layered Intrusion. AGU Fall Meeting Abstracts.

Goetze, H.J., Lahmeyer, B., 1988. Application of three-dimensional interactive modeling in gravity and magnetics. Geophysics 53, 1096–1108.

Golynsky, A.V., Ferraccioli, F., Hong, J.K., Golynsky, D.A., Frese, R.R.B., Young, D.A., Blankenship, D.D., Holt, J.W., Ivanov, S.V., Kiselev, A.V., Masolov, V.N., Eagles, G., Gohl, K., Jokat, W., Damaske, D., Finn, C., Aitken, A., Bell, R.E., Armadillo, E., Jordan, T.A., Greenbaum, J.S., Bozzo, E., Caneva, G., Forsberg, R., Ghidella, M., Galindo-Zaldivar, J., Bohoyo, F., Martos, Y.M., Nogi, Y., Quartini, E., Kim, H.R., Roberts, J.L., 2018. New magnetic anomaly map of the Antarctic. Geophys. Res. Lett. 45, 6437–6449.

Götze, H.-J., Schmidt, S., 2010. IGMAS+: a new 3D gravity, FTG and magnetic modelling software tool. In: Airborne Gravity 2010-Abstracts from the ASEG-PESA Airborne Gravity 2010 Workshop, pp. 91–96.

Himmelberg, G.R., Ford, A.B., 1977. Iron-titanium oxides of the Dufek Intrusion, Antarctica. Am. Mineral. 62, 623–633.

Jones, P.C., 2020. Processed Line Aerogravity Data over the Dufek Massif, Pensacola Mountains (1997/99 Season) (Version 1.0). UK Polar Data Centre, Natural Environment Research Council, UK Research & Innovation.

Jones, P.C., Johnson, A.C., 1995. Airborne gravity survey in southern Palmer Land, Antarctica. In: Schwarz, K.P., Brozena, J., Hein, G. (Eds.), Proceedings of IAG Symposium on Airborne Field Determination. Department of Geomatics Engineering at the University of Calgary, Calgary, Alberta, Canada, IUGG XXI General Assembly, Boulder, Colorado, pp. 117–123.

Jordan, T.A., Becker, D., 2018. Investigating the distribution of magmatism at the onset of Gondwana breakup with novel strapdown gravity and aeromagnetic data. Phys. Earth Planet. In. 282, 77–88.

Jordan, T.A., Ferraccioli, F., Ross, N., Corr, H.F.J., Leat, P.T., Bingham, R.G., Rippin, D. M., le Brocq, A., Siegert, M.J., 2013. Inland extent of the Weddell Sea Rift imaged by new aerogeophysical data. Tectonophysics 585, 137–160.

Jordan, T., Corr, H., Robinson, C., 2021. Processed Line Aeromagnetic Data from the FISS 2016 Surveys Covering the Filchner and Halley Ice Shelves, and the English Coast (western Palmer Land), West Antarctica (2016/2017) (Version 1.0). NERC EDS UK Polar Data Centre.

Kistler, R.W., White, L.D., Ford, A.B., 2000. Strontium and oxygen isotopic data and age for the layered gabbroic Dufek Intrusion, Antarctica. In: U.S. Dept. of the Interior, U. S. Geological Survey Open-File Report, 00-133, - ed, p. 29.

Minor, D.R., Mukasa, S.B., 1997. Zircon U-Pb and hornblende ^{40}Ar-^{39}Ar ages for the Dufek layered mafic intrusion, Antarctica: implications for the age of the Ferrar large igneous province. Geochim. Cosmochim. Acta 61, 2497–2504.

Morlighem, M., Rignot, E., Binder, T., Blankenship, D., Drews, R., Eagles, G., Eisen, O., Ferraccioli, F., Forsberg, R., Fretwell, P., Goel, V., Greenbaum, J.S., Gudmundsson, H., Guo, J., Helm, V., Hofstede, C., Howat, I., Humbert, A., Jokat, W., Karlsson, N.B., Lee, W.S., Matsuoka, K., Millan, R., Mouginot, J., Paden, J., Pattyn, F., Roberts, J., Rosier, S., Ruppel, A., Seroussi, H., Smith, E.C., Steinhage, D., Sun, B., Broeke, M.R.v.d., Ommen, T.D.v., Wessem, M.v., Young, D.A., 2020. Deep glacial troughs and stabilizing ridges unveiled beneath the margins of the Antarctic ice sheet. Nat. Geosci. 13, 132–137.

Mungall, J.E., Kamo, S.L., McQuade, S., 2016. U–Pb geochronology documents out-of-sequence emplacement of ultramafic layers in the Bushveld Igneous Complex of South Africa. Nat. Commun. 7, 13385.

Nelson, D., Cottle, J., Schoene, B., 2019. Butcher Ridge igneous complex: A glassy layered silicic magma distribution center in the Ferrar large igneous province, Antarctica. GSA Bull. 132.

Nielsen, T.F.D., 2004. The shape and volume of the Skaergaard Intrusion, Greenland: implications for mass balance and bulk composition. J. Petrol. 45, 507–530.

Peterson, D.E., Bedrosian, P.A., Finn, C.A., 2023. Subsurface Characterization of the Duluth Complex and Related Intrusions from 3D Modeling of Gravity and Magnetotelluric Data, Institute on Lake Superior Geology 69th Annual Meeting. Eau Claire, WI, Institute on Lake Superior Geology, p. 2.

Ranganai, R.T., Whaler, K.A., Ebinger, C.J., 2016. Aeromagnetic interpretation in the south-central Zimbabwe Craton: (reappraisal of) crustal structure and tectonic implications. Int. J. Earth Sci. 105, 2175–2201.

Salem, A., Williams, S., Fairhead, J.D., Ravat, D., Smith, R., 2007. Tilt-depth method: a simple depth estimation method using first-order magnetic derivatives. Lead. Edge 1502–1505.

Scoates, J.S., Wall, C.J., Friedman, R.M., Weis, D., Mathez, E.A., VanTongeren, J.A., 2021. Dating the bushveld complex: timing of crystallization, duration of magmatism, and cooling of the world's largest layered intrusion and related rocks. J. Petrol. 62, egaa107.

Semenov, V.S., Mikhailov, V.M., Koptev-Dvornikov, E.V., Ford, A.B., Shulyatin, O.G., Semenov, S.V., Tkacheva, D.A., 2014. Layered Jurassic Intrusions in Antarctica. Petrology 22, 547–573.

Storey, B.C., Macdonald, D.I.M., Dalziel, I.W.D., Isbell, J.L., Millar, I.L., 1996. Early Paleozoic sedimentation, magmatism, and deformation in the Pensacola Mountains, Antarctica: the significance of the Ross orogeny. Geol. Soc. Am. Bull. 108, 685–707. https://doi.org/10.1130/0016-7606(1996)1108<0685:EPSMAD>1132.1133.CO;1132.

The Polar Rock Repository (PRR), 2021. Polar rock and dredge samples available for research and educational use from the PRR. Byrd Polar and Climate Research Center (BPCRC), Ohio State University.

Tinto, K., Bell, R., Cochran, J.R., 2010. updated 2019. IceBridge Sander AIRGrav L1B Geolocated Free Air Gravity Anomalies, Version 1. NASA National Snow and Ice Data Center Distributed Active Archive Center, Boulder, Colorado USA.

VanTongeren, J.A., Zirakparvar, N.A., Mathez, E.A., 2016. Hf isotopic evidence for a cogenetic magma source for the Bushveld Complex and associated felsic magmas. Lithos 248-251, 469–477.

VanTongeren, J., Taylor, A., Schoene, B., 2020. Solidification timescale for the Dufek Intrusion, Antarctica determined by U-Pb zircon ages. In: EGU General Assembly 2020. EGU, Online.

von Frese, R.R.B., Hinze, W.J., Braile, L.W., Luca, A.J., 1981. Spherical earth gravity and magnetic anomaly modeling by Gauss- Legendre quadrature integration. J. Geophys. 49, 234–242.

Wilson, A.H., 1996. The great dyke of Zimbabwe. In: Cawthorn, R.G. (Ed.), Developments in Petrology. Elsevier, pp. 365–402.